Dark matter: scalar or vector?

Bohdan GRZADKOWSKI
University of Warsaw

Motivations

- There exists a simple model of Abelian vector dark matter (VDM), that implies an existence of two scalar degrees of freedom, h_1 (SM-like) and h_2 (non-SM-like), that mix through their mass matrix, with an angle α.

- The VDM is similar to a model of scalar dark matter (SDM), in which a DM candidate is an imaginary component (odd under stabilizing symmetry) of an extra complex scalar field added to the SM. The real component (even under stabilizing symmetry) develops a vacuum expectation value and mixes with the SM Higgs doublet, so there are also two scalar degrees of freedom, h_1 (SM-like) and h_2 (non-SM-like), that mix through their mass matrix, with an angle α.

- This project is an attempt to investigate if it is possible to distinguish the two models. In other words we are seeking measurements that could be performed in near future that could disentangle the two models.

Vector versus scalar dark matter

Bohdan GRZADKOWSKI
University of Warsaw

- Motivations
- Vector dark matter (VDM) model
- Scalar dark matter (SDM) model
- Direct detection
- ILC signals
- Scans over parameters spaces
- Summary

◇ D. Azevedo, M. Duch, BG, D. Huang, M. Iglicki, R. Santos, "Testing scalar versus vector dark matter", arXiv:1808.01598,
◇ D. Azevedo, M. Duch, BG, D. Huang, M. Iglicki, R. Santos, "Natural suppression of dark-matter-nucleon scattering", in progress,
◇ M. Duch, BG, M. McGarrie, "A stable Higgs portal with vector dark matter", JHEP 1509 (2015) 162

The Vector Dark Matter (VDM) model

- T. Hambye, "Hidden vector dark matter", JHEP 0901 (2009) 028,
- O. Lebedev, H. M. Lee, and Y. Mambrini, "Vector Higgs-portal dark matter and the invisible Higgs", Phys.Lett. B707 (2012) 570,
- Y. Farzan and A. R. Akbarieh, "VDM: A model for Vector Dark Matter", JCAP 1210 (2012) 026,
- S. Baek, P. Ko, W.-I. Park, and E. Senaha, "Higgs Portal Vector Dark Matter : Revisited", JHEP 1305 (2013) 036,
- Ch. Gross, O. Lebedev, Y. Mambrini, "Non-Abelian gauge fields as dark matter", arXiv:1505.07480,
- ...

The model:

- extra $U(1)_X$ gauge symmetry (A_X^μ),
- a complex scalar field S, whose vev generates a mass for the $U(1)$'s vector field, $S = (0, \mathbf{1}, \mathbf{1}, 1)$ under $U(1)_Y \times SU(2)_L \times SU(3)_c \times U(1)_X$.
- SM fields neutral under $U(1)_X$,
- in order to ensure stability of the new vector boson a $\mathbb{Z}_2$ symmetry is assumed to forbid $U(1)$-kinetic mixing between $U(1)_X$ and $U(1)_Y$. The extra gauge boson A_μ and the scalar S field transform under $\mathbb{Z}_2$ as follows

$$A_X^\mu \xrightarrow{C} -A_X^\mu \ , \ S \xrightarrow{C} S^*$$

The scalar potential

$$V = -\mu_H^2 |H|^2 + \lambda_H |H|^4 - \mu_S^2 |S|^2 + \lambda_S |S|^4 + \kappa |S|^2 |H|^2.$$

The vector bosons masses:

$$m_W = \frac{1}{2} g v, \quad m_Z = \frac{1}{2}\sqrt{g^2 + g'^2} v \quad \text{and} \quad m_X = g_X v_S,$$

where

$$\langle H \rangle = \begin{pmatrix} 0 \\ \frac{v}{\sqrt{2}} \end{pmatrix} \text{ and } \langle S \rangle = \frac{v_S}{\sqrt{2}}$$

Positivity of the potential implies

$$\lambda_H > 0, \quad \lambda_S > 0, \quad \kappa > -2\sqrt{\lambda_H \lambda_S}.$$

The minimization conditions for scalar fields

$$(2\lambda_H v^2 + \kappa v_S^2 - 2\mu_H^2) v = 0 \text{ and } (\kappa v^2 + 2\lambda_S v_S^2 - 2\mu_S^2) v_S = 0$$

For $\kappa^2 < 4\lambda_H\lambda_S$ the global minimum is

$$v^2 = \frac{4\lambda_S\mu_H^2 - 2\kappa\mu_S^2}{4\lambda_H\lambda_S - \kappa^2} \quad \text{and} \quad v_S^2 = \frac{4\lambda_H\mu_S^2 - 2\kappa\mu_H^2}{4\lambda_H\lambda_S - \kappa^2}$$

Both scalar fields can be expanded around corresponding vev's as follows

$$S = \frac{1}{\sqrt{2}}(v_S + \phi_S + i\sigma_S) \quad , \quad H^0 = \frac{1}{\sqrt{2}}(v + \phi_H + i\sigma_H) \quad \text{where} \quad H = \begin{pmatrix} H^+ \\ H^0 \end{pmatrix}.$$

The mass squared matrix $\mathcal{M}^2$ for the fluctuations (ϕ_H, ϕ_S) and their eigenvalues read

$$\begin{aligned} \mathcal{M}^2 &= \begin{pmatrix} 2\lambda_H v^2 & \kappa v v_S \\ \kappa v v_S & 2\lambda_S v_S^2 \end{pmatrix} \\ m_\pm^2 &= \lambda_H v^2 + \lambda_S v_S^2 \pm \sqrt{\lambda_S^2 v_S^4 - 2\lambda_H\lambda_S v^2 v_S^2 + \lambda_H^2 v^4 + \kappa^2 v^2 v_S^4} \end{aligned}$$

$$\mathcal{M}^2_{\mathsf{diag}} = \begin{pmatrix} m_1^2 & 0 \\ 0 & m_2^2 \end{pmatrix}, \quad R = \begin{pmatrix} \cos\alpha & -\sin\alpha \\ \sin\alpha & \cos\alpha \end{pmatrix}, \quad \begin{pmatrix} h_1 \\ h_2 \end{pmatrix} = R^{-1} \begin{pmatrix} \phi_H \\ \phi_S \end{pmatrix},$$

Scalar dark matter (SDM) model

V. Silveira, A. Zee, "Scalar Phantoms", Phys. Lett. B 161, 136 (1985),
J. McDonald, "Gauge singlet scalars as cold dark matter", Phys. Rev. D50 (1994) 36373649, [hep-ph/0702143]

$$V = -\mu_H^2|H|^2 + \lambda_H|H|^4 - \mu_S^2|S|^2 + \lambda_S|S|^4 + \kappa|S|^2|H|^2 + \mu^2(S^2 + S^{*\,2})$$

Positivity: $\lambda_H > 0, \quad \lambda_S > 0, \quad \kappa > -2\sqrt{\lambda_H \lambda_S}$
Symmetries:

- $S = \frac{1}{\sqrt{2}}(v_S + \phi_S + iA)$, with $\langle S \rangle = \frac{v_S}{\sqrt{2}}$,
- Stability of the imaginary part of S: $S \xrightarrow{C} S^*$, ($\phi_S \to \phi_S$ and $A \to -A$),
- $U(1)$ softly broken by $\mu^2(S^2 + S^{*\,2}) \quad \Longrightarrow \quad$ would be pseudo-Goldstone boson (A).

The global minimum:

$$v^2 = \frac{4\lambda_S \mu_H^2 - 2\kappa(\mu_S^2 - 2\mu^2)}{4\lambda_H\lambda_S - \kappa^2}, \quad v_S^2 = \frac{4\lambda_H(\mu_S^2 - 2\mu^2) - 2\kappa\mu_H^2}{4\lambda_H\lambda_S - \kappa^2}, \quad v_A^2 = 0$$

$$V_1 = \frac{-1}{4\lambda_H\lambda_S - \kappa^2}\left\{\lambda_H(\mu_S^2 - 2\mu^2)^2 + \mu_H^2\left[\lambda_S\mu_H^2 - \kappa(\mu_S^2 - 2\mu^2)\right]\right\}$$

$$\mathcal{M}^2 = \begin{pmatrix} 2\lambda_H v^2 & \kappa v v_S & 0 \\ \kappa v v_S & 2\lambda_S v_S^2 & 0 \\ 0 & 0 & -4\mu^2 \end{pmatrix}$$

$2\lambda_S\mu_H^2 > \kappa(\mu_S^2 - 2\mu^2)$ and $2\lambda_H(\mu_S^2 - 2\mu^2) > \kappa\mu_H^2$ and $\mu^2 < 0$

Direct detection

The DM direct detection signals are naturally suppressed in the SDM model.

$$V \supset \frac{A^2}{2}(2\lambda_S v_S \phi_S + \kappa v \phi_H) = \frac{A^2}{2v_S}(\sin\alpha\, m_1^2 h_1 + \cos\alpha\, m_2^2 h_2)\,,$$

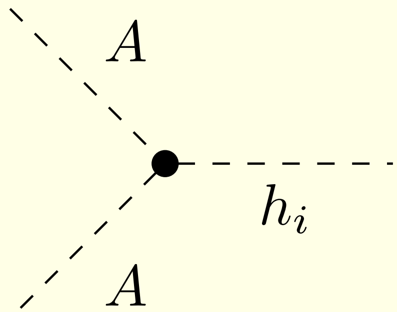

$$= -iR_{2i}\frac{m_i^2}{v_S}$$

The corresponding amplitude for the spin-independent DM nuclear recoils reads:

$$\begin{aligned} i\mathcal{M} &= -i\frac{\sin 2\alpha f_N m_N}{2vv_S}\left(\frac{m_1^2}{q^2-m_1^2}-\frac{m_2^2}{q^2-m_2^2}\right)\bar{u}_N(p_4)u_N(p_2) \\ &\approx -i\frac{\sin 2\alpha f_N m_N}{2vv_S}\left(\frac{m_1^2-m_2^2}{m_1^2 m_2^2}\right)q^2\bar{u}_N(p_4)u_N(p_2)\,. \end{aligned}$$

$$S = \frac{1}{\sqrt{2}}(v_s + \phi_S)e^{iA/v_s}\,,$$

- A is odd under the Z_2 symmetry transformation $S \leftrightarrow S^*$, it is DM candidate.

- The only terms that contain A are the kinetic and the $U(1)$ symmetry softly-breaking terms:

$$\begin{aligned}\mathcal{L}_A &= \partial^\mu S^* \partial_\mu S - \frac{M^3}{\sqrt{2}}(S + S^*) - \mu^2(S^2 + S^{*2}) \\ &\supset \frac{1}{2}\partial^\mu A \partial_\mu A + \frac{1}{2}\left(4\mu^2 + \frac{M^3}{v_s}\right)A^2 + \frac{\phi_S}{v_s}\partial^\mu A \partial_\mu A + \left(\frac{4\mu^2}{v_s} + \frac{M^3}{2v_s^2}\right)\phi_S A^2\,,\end{aligned}$$

so $m_A^2 = -4\mu^2 - M^3/v_s$.

- Repeatedly integrating by parts and adopting free equations of motion for A and h_i, one finds the pseudo-Goldstone-Higgs vertices as follows

$$\mathcal{L}_A \supset \frac{1}{2}(\partial^\mu A \partial_\mu A - m_A^2 A^2) - \frac{R_{2i}}{2v_s}\left(m_i^2 + \frac{M^3}{v_S}\right)h_i A^2$$

The total cross section σ_{AN}:

$$\sigma_{AN}^{(tree)} \approx \frac{\sin^2 2\alpha\, f_N^2}{3\pi}\frac{m_N^2}{m_A^2}\frac{\mu_{AN}^6}{v^2 v_S^2}\frac{(m_1^2 - m_2^2)^2}{m_1^4 m_2^4} v_A^4\,,$$

where $\mu_{AN} = m_A m_N/(m_A + m_N)$ is the reduced mass in the DM-nucleon system, and v_A is the A velocity in the lab frame. Since $v_A \sim 200\ \mathrm{km/s}$, the total DM nuclear recoil cross section σ_{AN} is greatly suppressed by the factor $v_A^4 \sim 10^{-13}$:

$$\sigma_{AN}^{(tree)} \sim 10^{-70}\ \mathrm{cm}^2 \ll \sigma_{AN}^{(\mathrm{X}ENON1T)} \sim 10^{-46}\ \mathrm{cm}^2$$

C. Gross, O. Lebedev, and T. Toma, "Cancellation Mechanism for Dark-Matter-Nucleon Interaction", Phys. Rev. Lett. 119 (2017), no. 19 191801, [arXiv:1708.02253].

$$\sigma_{AN} \approx \frac{\sin^2\alpha}{64\pi^5}\frac{m_N^4 f_N^2}{m_1^4 v^2}\frac{m_2^4 m_A^2}{v_S^6}\begin{cases} \left(\frac{m_2}{m_A}\right)^4, & m_A \geq m_2 \\ 1\,, & m_A < m_2 \end{cases}$$

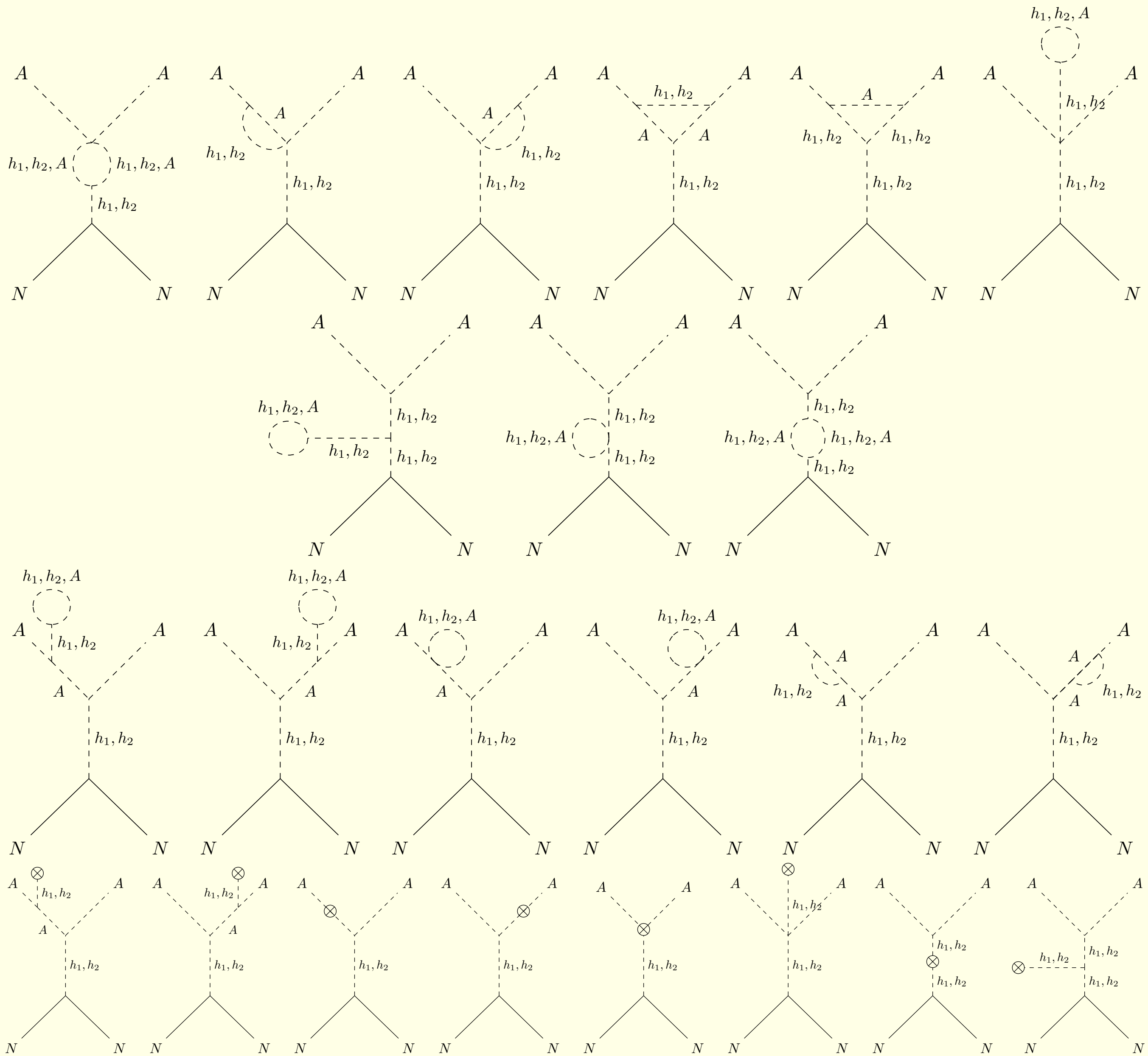

Figure 1: 1-loop diagrams contributing to A-nucleon scattering.

ILC signals

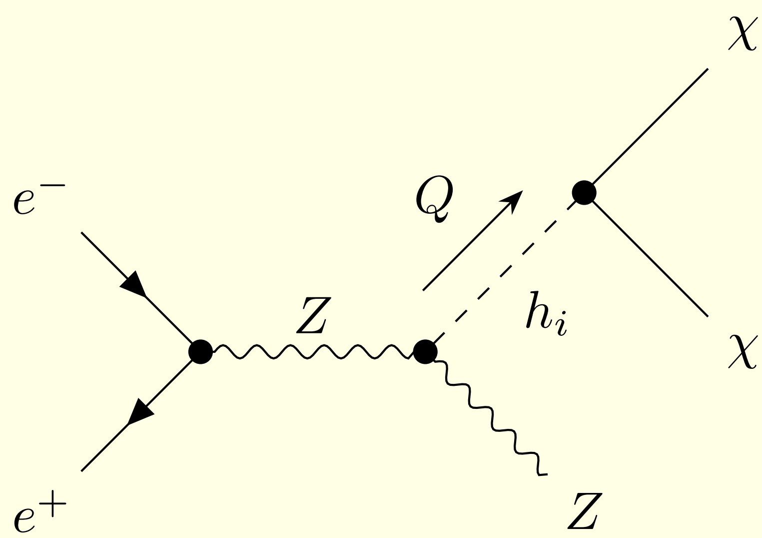

Figure 2: Feynman diagram for $e^+e^- \to Z\chi\bar{\chi}$, χ denotes the dark particle ($\chi = A, X$).

- P. Ko, H. Yokoya, "Search for Higgs portal DM at the ILC", JHEP 1608 (2016) 109,

- T. Kamon, P. Ko, J. Li "Characterizing Higgs portal dark matter models at the ILC", Eur.Phys.J. C77 (2017) no.9, 652

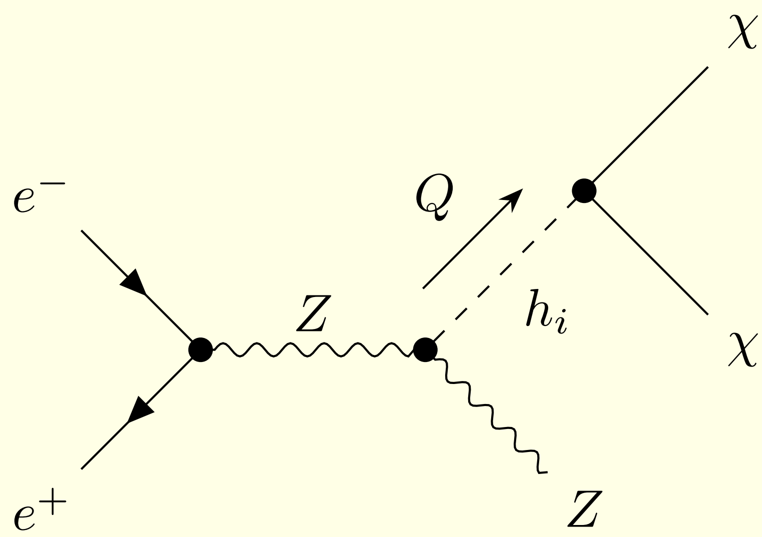

Figure 3: Feynman diagram for $e^+e^- \to Z\chi\bar{\chi}$, χ denotes the dark particle ($\chi = A, X$).

$$\frac{d\sigma}{dE_Z}(E_Z) = f(s, E_Z) \cdot \frac{\left(\frac{\sin 2\alpha}{v_S}\right)^2 \cdot \sqrt{1 - 4\frac{m_{DM}^2}{Q^2}} \cdot (m_1^2 - m_2^2)^2 \cdot Q^4}{\left[(Q^2 - m_1^2)^2 + (m_1\Gamma_1)^2\right]\left[(Q^2 - m_2^2)^2 + (m_2\Gamma_2)^2\right]} \times$$

$$\times \begin{cases} 1 & \text{(SDM)} \\ 1 - 4\frac{m_X^2}{Q^2} + 12\left(\frac{m_X^2}{Q^2}\right)^2 & \text{(VDM)} \end{cases},$$

$$\frac{2}{3} \leq 1 - 4\frac{m_X^2}{Q^2} + 12\left(\frac{m_X^2}{Q^2}\right)^2 \leq 1$$

$$Q^2 = s - 2E_Z\sqrt{s} + m_Z^2$$

$$f(s, E_Z) \equiv \frac{g_v^2 + g_a^2}{12 \cdot (2\pi)^3} \sqrt{E_Z^2 - m_Z^2} \left(2m_Z^2 + E_Z^2\right) \left(\frac{g^2}{\cos\theta_W^2} \frac{1}{s - m_Z^2}\right)^2$$

$$Q^2 = Q^2(s, E_Z) \equiv s - 2E_Z\sqrt{s} + m_Z^2$$

$$E_Z(Q^2 = m_i^2) = E_i \equiv \frac{s - m_i^2 + m_Z^2}{2\sqrt{s}}.$$

$$E_{\max} = \frac{s - 4m_{DM}^2 + m_Z^2}{2\sqrt{s}},$$

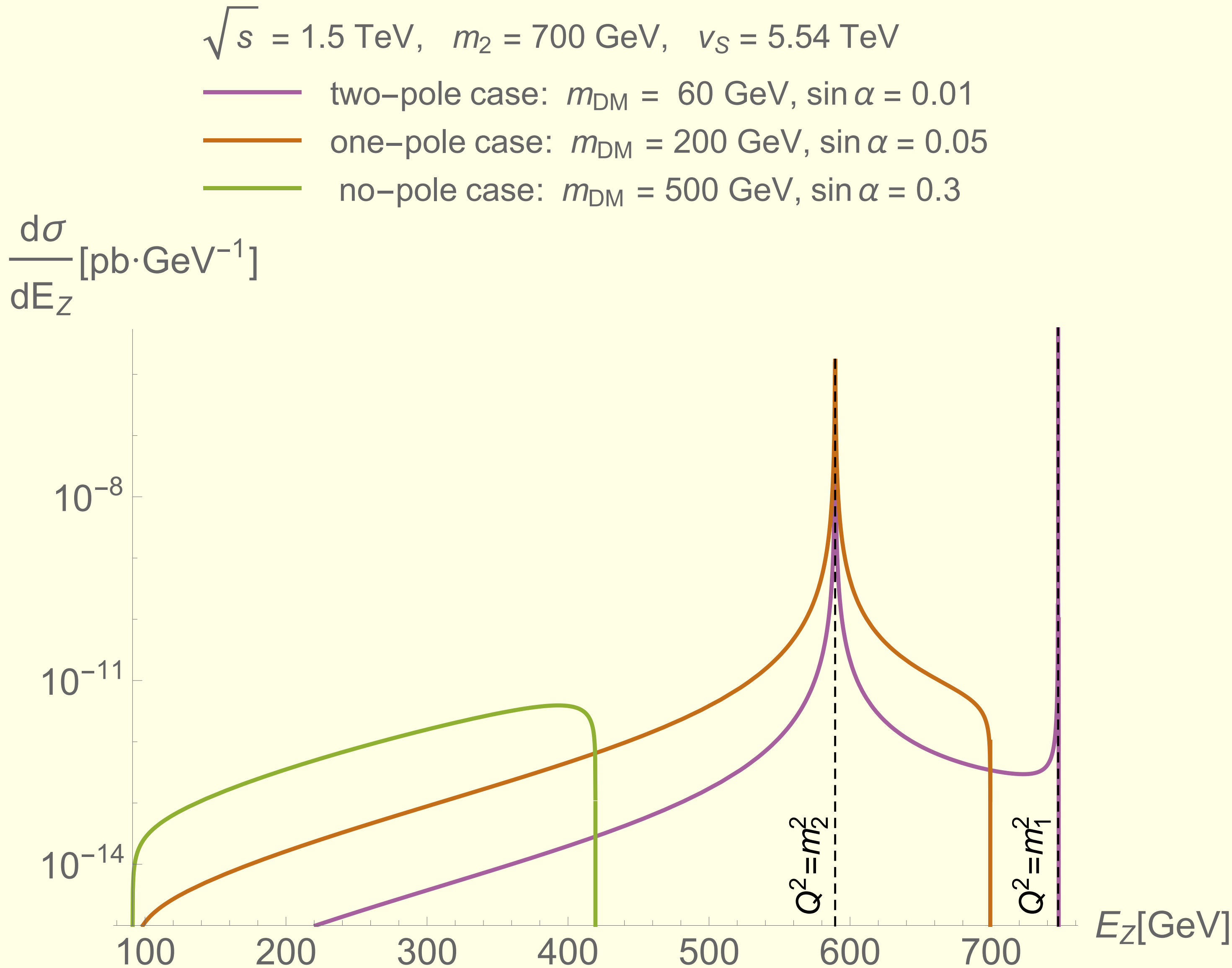

Figure 4: $\frac{d\sigma}{dE_Z}$ for the SDM model.

$$E_Z(Q^2 = m_i^2) = E_i \equiv \frac{s - m_i^2 + m_Z^2}{2\sqrt{s}}, \qquad E_{\max} = \frac{s - 4m_{DM}^2 + m_Z^2}{2\sqrt{s}}$$

The strategy:

1. From the endpoint $E_{\max}$ one can determine m_{DM}:

$$E_{\max} = \frac{s - 4m_{DM}^2 + m_Z^2}{2\sqrt{s}},$$

2. In the presence of two poles, m_2 could be determined:

$$E_Z(Q^2 = m_2^2) = E_2 \equiv \frac{s - m_2^2 + m_Z^2}{2\sqrt{s}}.$$

3. Then ratio

$$1 \quad \leq \quad \frac{\frac{d\sigma_{\mathsf{SDM}}}{dE_Z}}{\frac{d\sigma_{\mathsf{VDM}}}{dE_Z}} \quad \leq \quad \frac{3}{2}$$

is uniquely determined. It is always greater than 1.

4. If $m_i^2 \simeq 6m_X^2$ the maximal deviation (50%) appears exactly at the i-th pole.

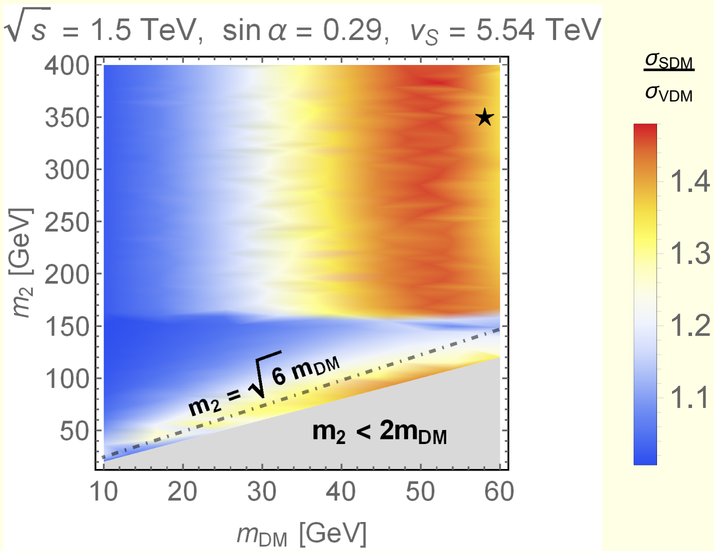

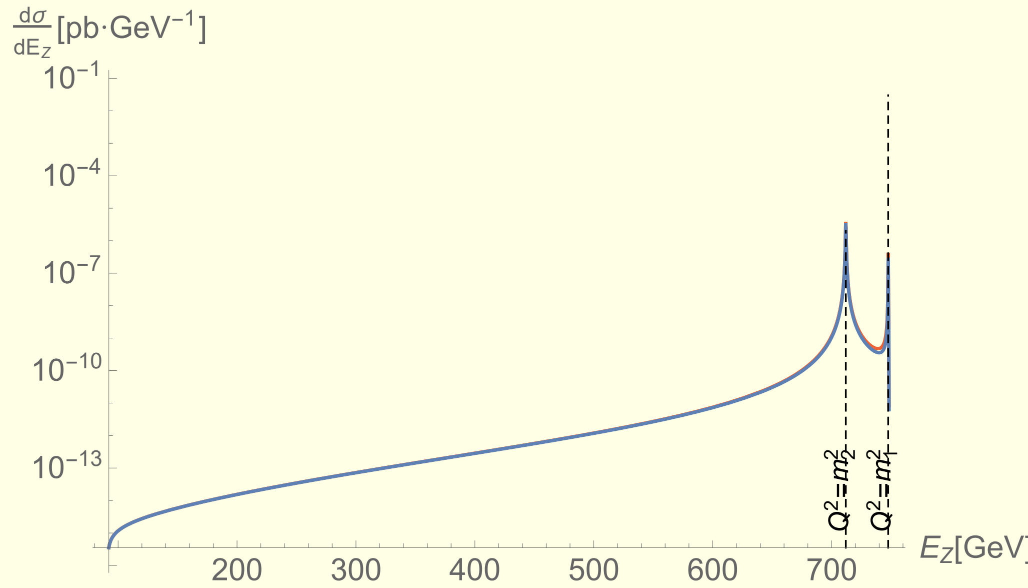

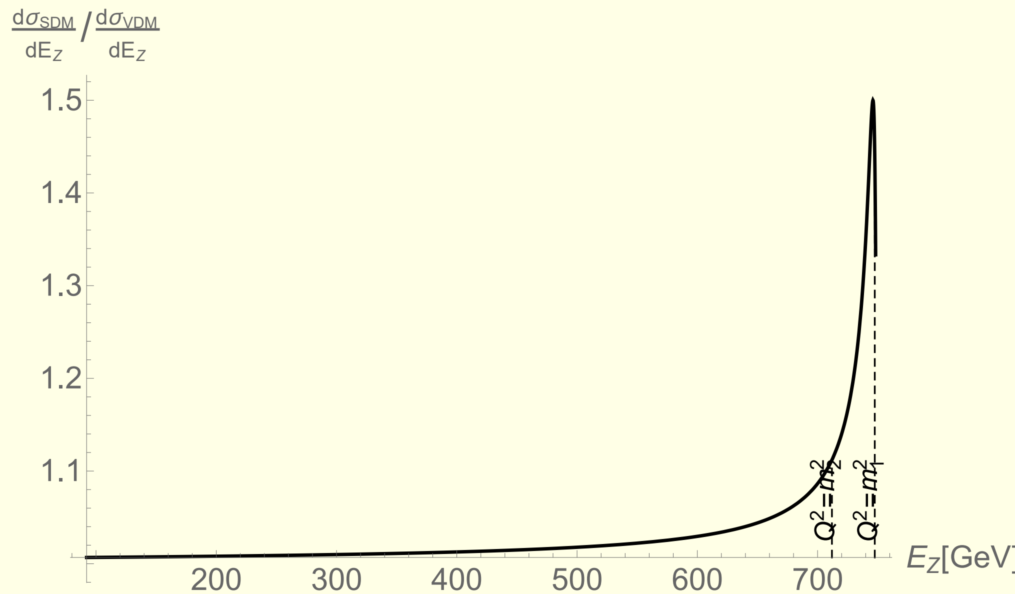

values in ★

m_2 = 350 GeV, m_{DM} = 58 GeV

scalar DM model: $\sigma_{tot} = 3.1\times10^{1}$ ab

$\Gamma_1 = 3.6\times10^{-3}$ GeV, $BR_{h_1\to DM}$ = 0.6 %

Γ_2 = 1.8 GeV, $BR_{h_2\to DM}$ = 0.7 %

vector DM model: $\sigma_{tot} = 2.2\times10^{1}$ ab

$\Gamma_1 = 3.6\times10^{-3}$ GeV, $BR_{h_1\to DM}$ = 0.4 %

Γ_2 = 1.8 GeV, $BR_{h_2\to DM}$ = 0.6 %

$$\frac{d\sigma}{dE_Z} \propto \frac{\sqrt{1-4\frac{m_{DM}^2}{Q^2}}\cdot Q^4}{[(Q^2-m_1^2)^2+(m_1\Gamma_1)^2]\,[(Q^2-m_2^2)^2+(m_2\Gamma_1)^2]} \begin{cases} 1 & \text{(SDM)} \\ 1-4\frac{m_X^2}{Q^2}+12\left(\frac{m_X^2}{Q^2}\right)^2 & \text{(VDM)} \end{cases}$$

case	$\sqrt{s}$ [TeV]	$\sin\alpha$	v_S [TeV]	m_2 [GeV]	m_{DM} [GeV]	$\sigma_{\text{SDM}} - \sigma_{\text{VDM}}$ [ab]	$\Delta(\sigma_{\text{SDM}} - \sigma_{\text{VDM}})$ [ab]	$\frac{\Delta(\sigma_{\text{SDM}}-\sigma_{\text{VDM}})}{\sigma_{\text{SDM}}-\sigma_{\text{VDM}}}$
two-pole	1.5 3.0	0.29	5.54	350	58	9 2.2	5.9 2.6	66 % 117 %
one-pole	1.5 3.0	0.3	2.04	630	287	1.3 0.5	2.1 1.16	165 % 232 %
no-pole	1.5 3.0	0.12	0.1	70	123	0.009 0.0023	0.2 0.0891	2089 % 3877 %

Table 1: Values of the parameters and corresponding uncertainties for the difference between the total cross-sections for the both models for $\sqrt{s} = 1.5$ TeV and $\sqrt{s} = 3$ TeV colliders at points marked by ,,$\star$".

Scans over parameter spaces

Independent parameters: $v_S, \sin\alpha, m_2$ and m_{DM} (m_A or m_X).

Parameter	Range
Second Higgs - m_2	[1,1000] GeV
Dark Matter - m_{DM}	[1,1000] GeV
Singlet VEV - v_s	[1,10^7] GeV
Mixing angle - α	[$-\frac{\pi}{4}$,$\frac{\pi}{4}$]

Table 2: Scan regions for independent parameter's for both models.

Collider constraints:

- The points are generated by the code `ScannerS` [R. Coimbra, M. O. P. Sampaio, and R. Santos, “ScannerS: Constraining the phase diagram of a complex scalar singlet at the LHC”, Eur. Phys. J. C73 (2013) 2428]:
  - the potential has to be bounded from below,
  - the vacuum is chosen so that the minimum is the global one,
  - perturbative unitarity holds.

- The bound on the signal strength μ is used to constraint $\cos\alpha$,

- $BR(h_1 \to \text{inv}) < 24\%$,

- S, T and U,

- The collider bounds from LEP, Tevatron and the LHC are imposed via `HiggsBounds` [P. Bechtle, O. Brein, S. Heinemeyer, G. Weiglein, and K. E. Williams, “HiggsBounds: Confronting Arbitrary Higgs Sectors with Exclusion Bounds from LEP and the Tevatron”,Comput. Phys. Commun. 181 (2010) 138] that provides 95% CL exclusion limits for all available searches for non-standard Higgs bosons.

Cosmological constraints:

- DM abundance: $(\Omega h^2)^{\rm obs}_{\rm DM} = 0.1186 \pm 0.002$ from Planck Collaboration, here we require that $(\Omega\, h^2)_{A,X} < 0.1186$ or we adopt 5σ allowed region,

- Direct detection: we apply the latest XENON1T upper bounds for the DM mass greater than 6 GeV, while for lighter DM particles, the combined limits from CRESST-II and CDMSlite are utilized for $\sigma^{\rm eff}_{AN,XN} \equiv f_{A,X}\sigma_{AN,XN}$, with

$$f_{A,X} = \frac{(\Omega h^2)_{A,X}}{(\Omega h^2)^{\rm obs}_{\rm DM}}\,,$$

  where $(\Omega h^2)_{A,X}$ is the calculated DM relic abundance for the SDM (A) or the VDM (X).

- Indirect detection: for the DM mass range of interest, the Fermi-LAT upper bound on the DM annihilations from dwarfs is the most stringent. We use the Fermi-LAT bound on $b\bar{b}$ when $m_{A,X} \geqslant m_b$, and that on light quarks for $m_{A,X} < m_b$.

DM decays of the Higgs bosons: $h_i \to XX$ and $h_i \to AA$

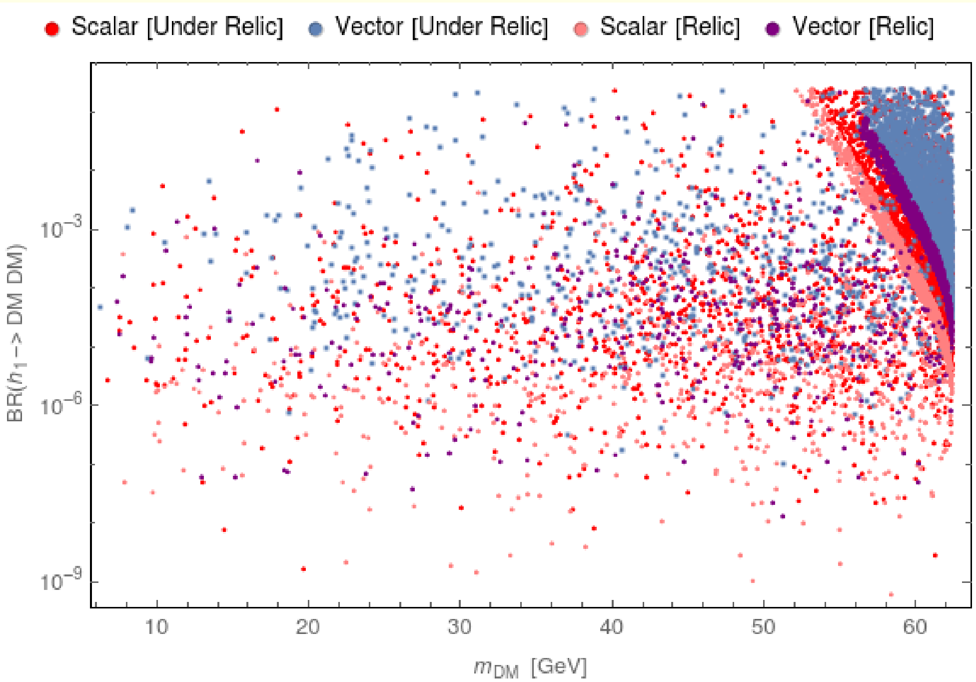

(a) $h_1 \to XX$ (VDM) and $h_1 \to AA$ (SDM).

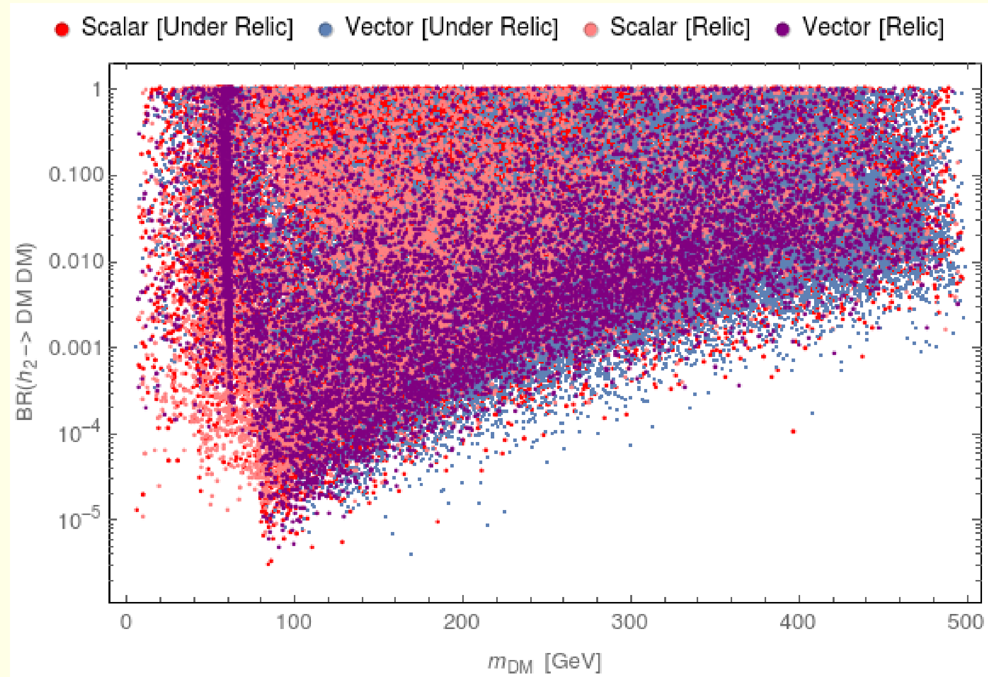

(b) $h_2 \to XX$ (VDM) and $h_2 \to AA$ (SDM).

Figure 5: Branching ratios of the SM-like Higgs (a) and of the second Higgs (b) into DM particles versus the dark matter mass m_{DM}. The colours are superimposed in the following order: red, blue, pink and then purple (so for instance a red dot may be hidden behind a blue dot).

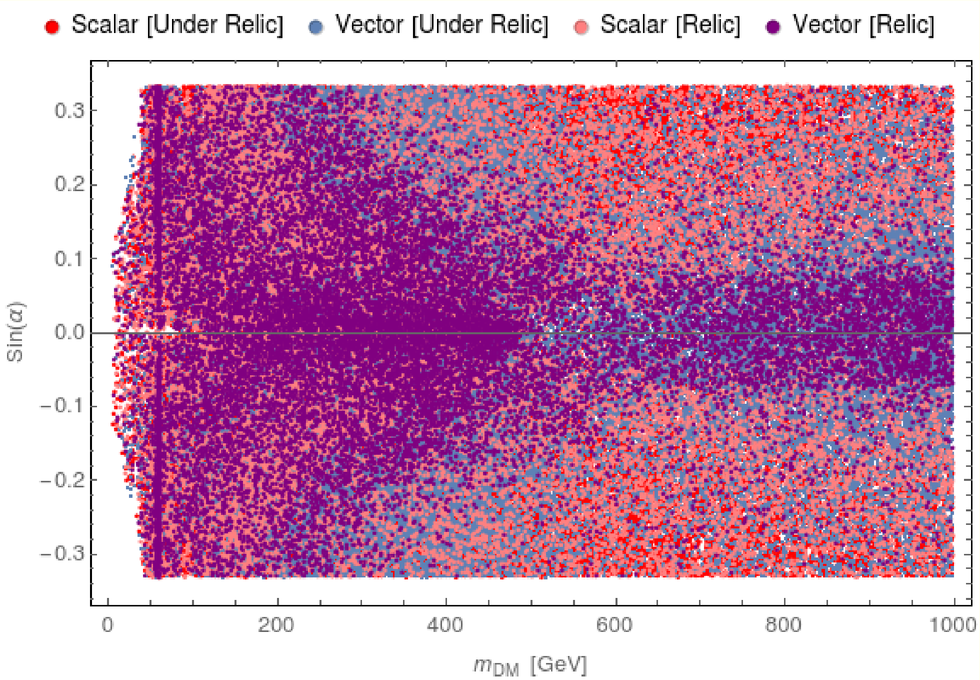

(a) $\sin\alpha$ versus m_{DM}.

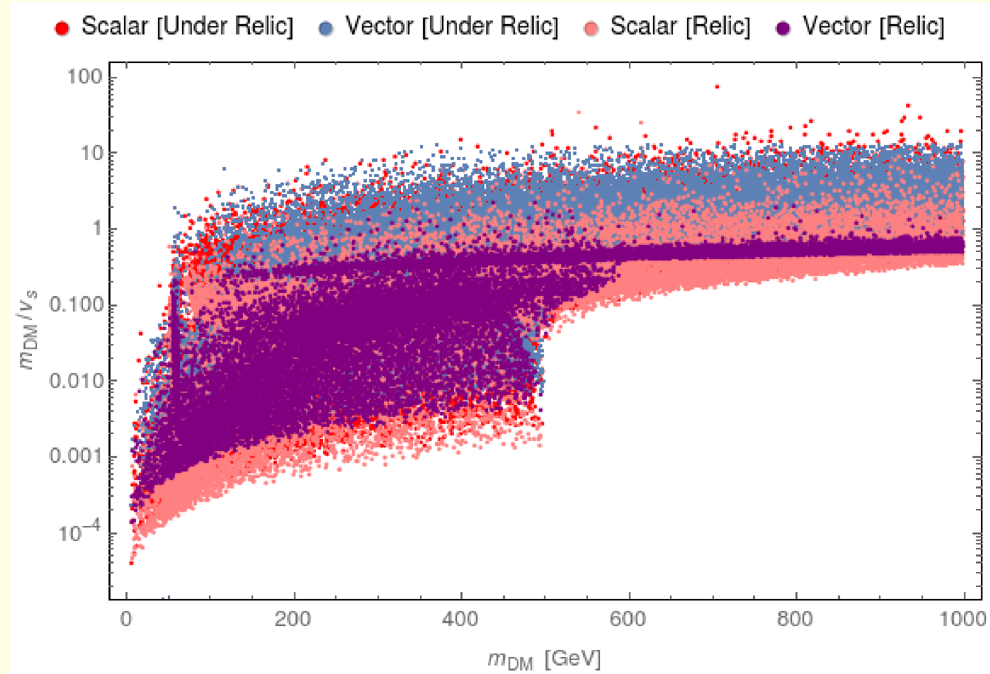

(b) m_{DM}/v_S versus m_{DM}.

Figure 6: $\sin\alpha$ (a) and m_{DM}/v_S (b) versus the dark matter mass m_{DM}.

$$\frac{m_{DM}}{v_s} = \begin{cases} g_X & \text{for VDM} \\ \frac{m_A}{v_S} & \text{for SDM} \end{cases}$$

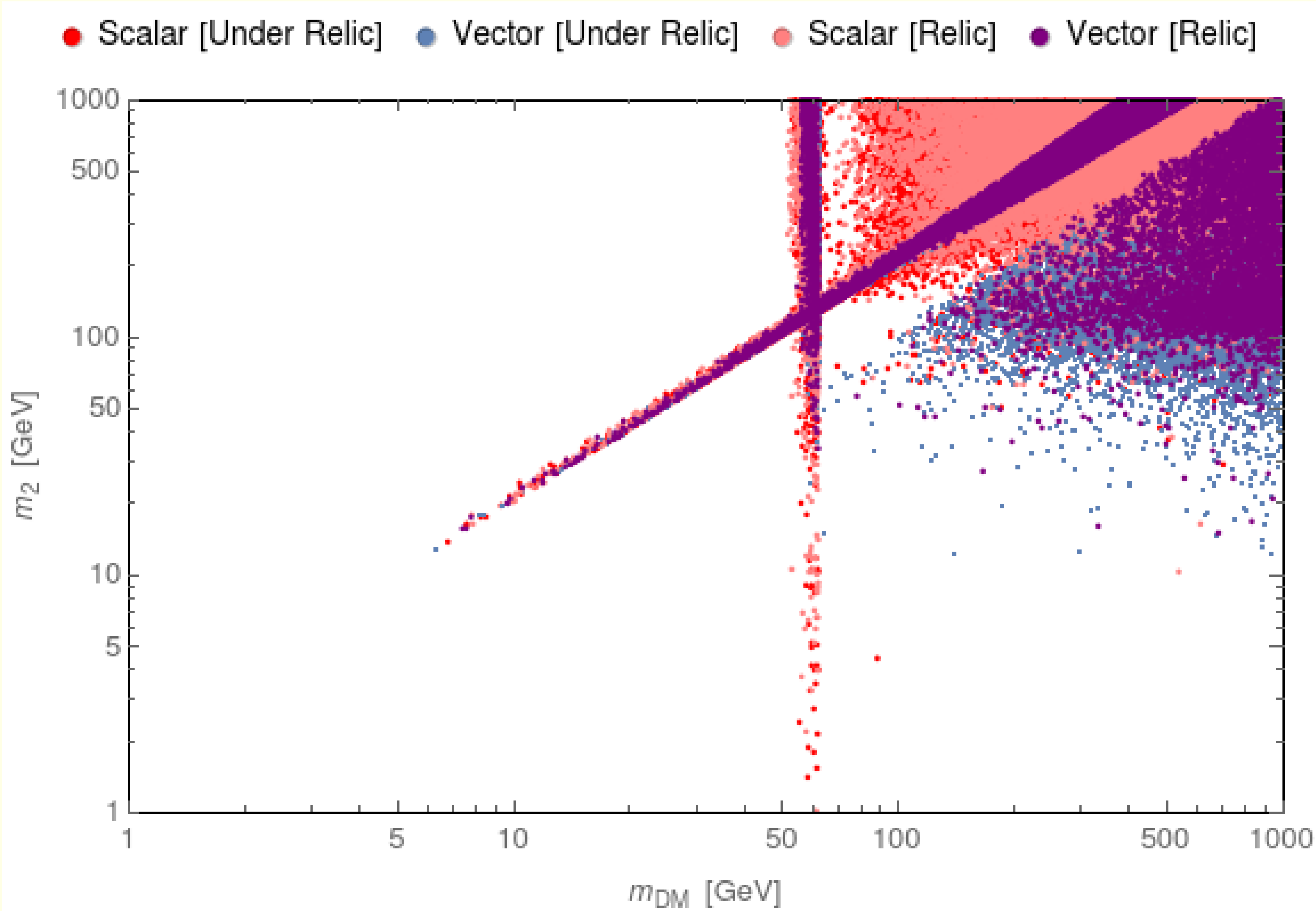

Figure 7: m_2 versus m_{DM}.

Where the models coexist:

- $m_2 \simeq 2m_{DM}$ (DM annihilation through the non-SM-like resonance h_2),
- $m_{DM} \simeq m_1/2$ (DM annihilation through the SM-like resonance h_1),

SDM and VDM could be disentangled by a measurement of m_{DM} and m_2.

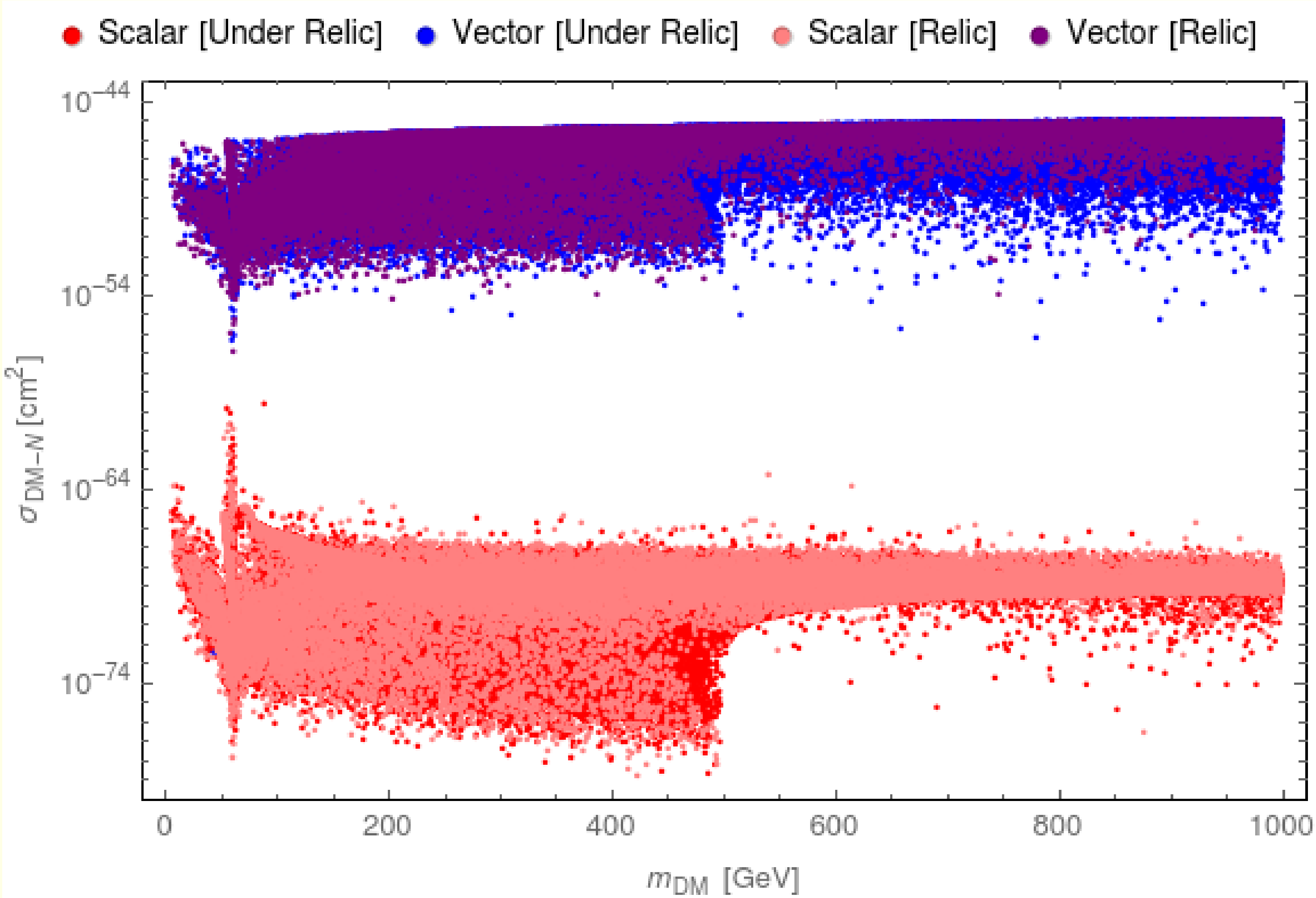

Figure 8: Dark matter-nucleon cross section versus m_{DM}.

- Suppression of σ_{DM-N} for the SDM model,
- h_1 and h_2 resonance effects for both the SDM and the VDM models, $m_1 \simeq 2m_{DM}$ and $m_2 \simeq 2m_{DM}$, respectively.

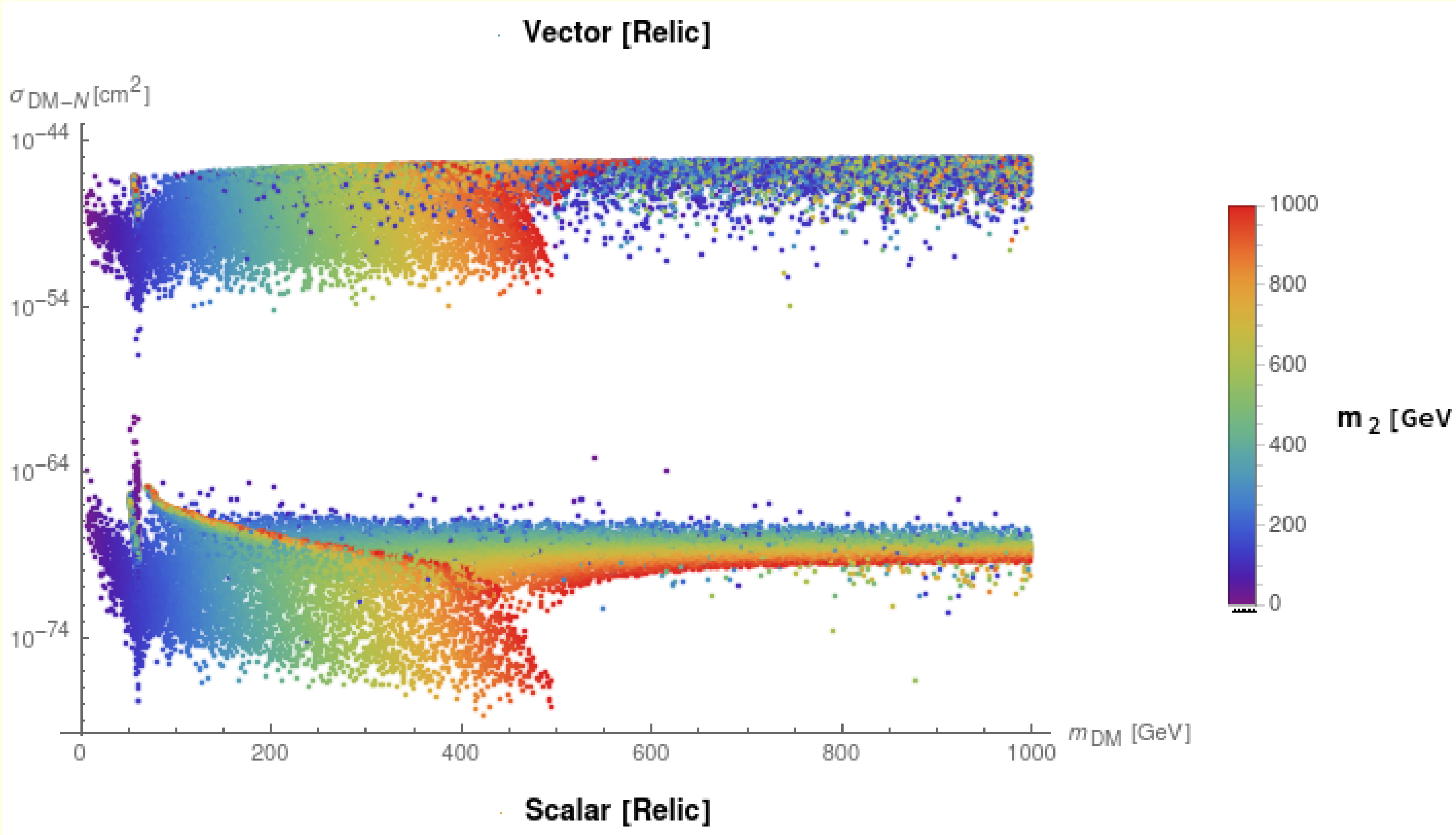

Figure 9: Dark matter-nucleon cross section versus m_{DM} colored with respect to m_2. DM abundance is within 5σ of experimental value.

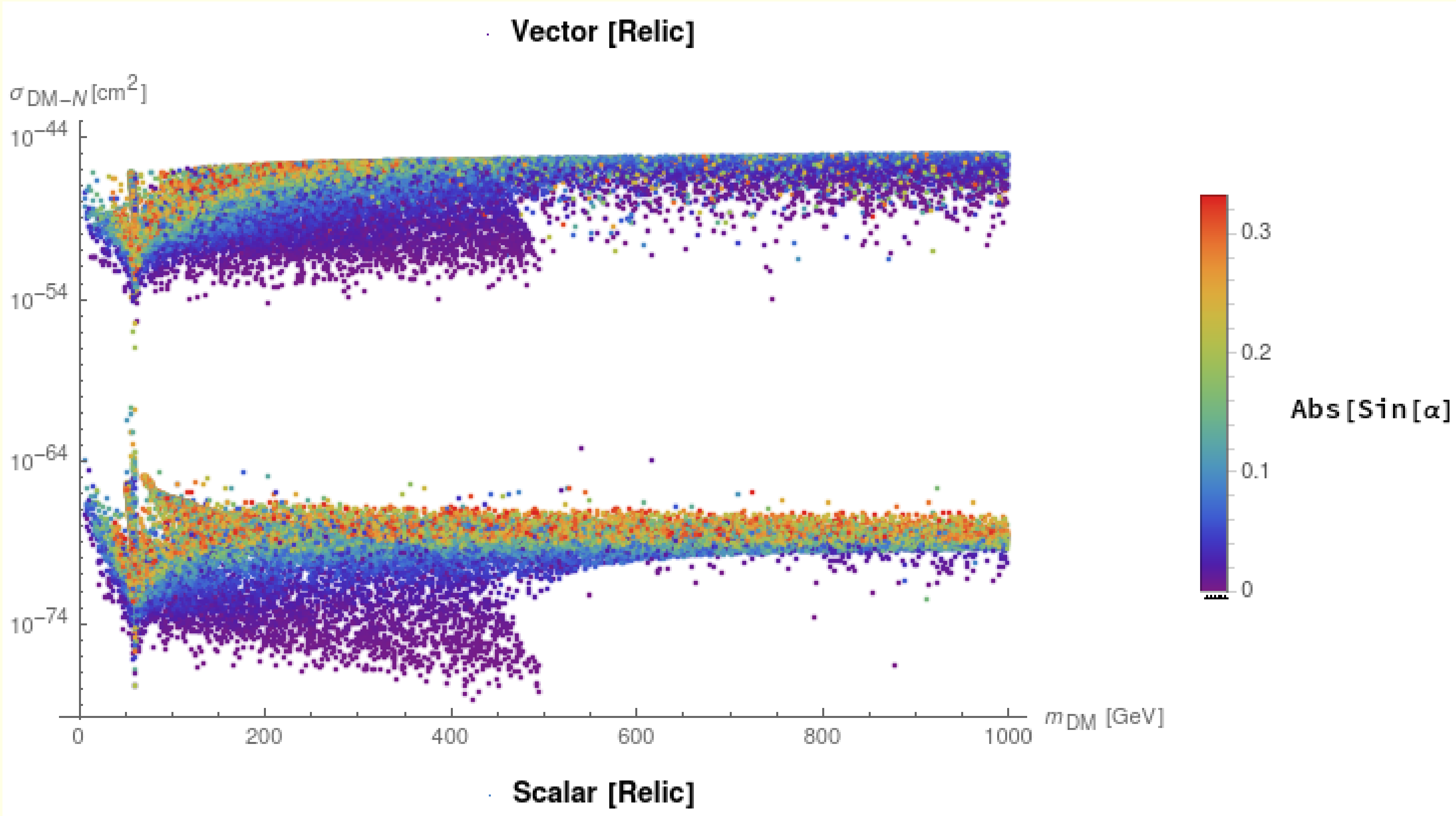

Figure 10: Dark matter-nucleon cross section versus m_{DM} colored with respect to $\sin\alpha$. DM abundance is within 5σ of experimental value.

Summary

Some preliminary conclusions:

1. The Abelian VDM model is challenged by a similar SDM model with DM candidate A that is a pseudo-Goldstone boson related to softly broken $U(1)$, by $\mu^2(S^2 + S^{*2})$,

2. Direct detection efficiently suppressed in the SDM model, $\sigma_{DM-N} \propto v_A^4$, as a consequence of A being a pseudo-Goldstone boson, 1-loop results adopted,

3. In some regions of (m_i, m_X) space $(m_i^2 \simeq 6m_X^2)$ the ILC might be useful to disentangle the models,

4. There exist regions in the parameter space of the models where only VDM could be realized.

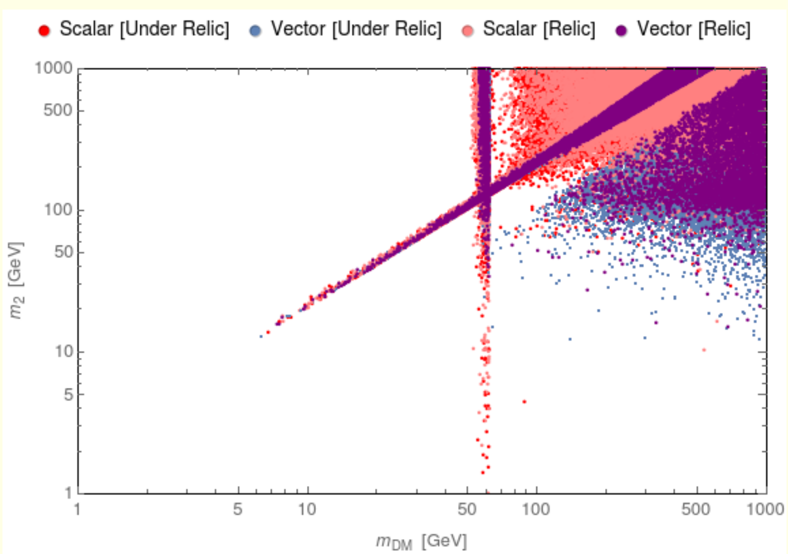

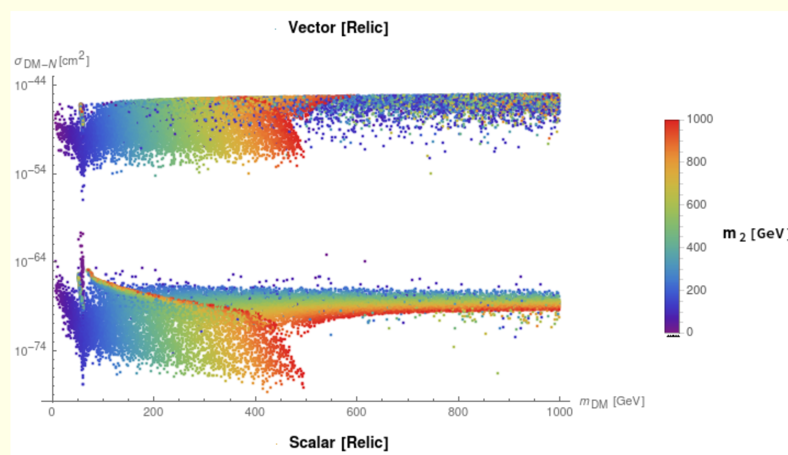

Vacuum stability

$$V = -\mu_H^2|H|^2 + \lambda_H|H|^4 - \mu_S^2|S|^2 + \lambda_S|S|^4 + \kappa|S|^2|H|^2$$

2-loop running of parameters adopted

$$\lambda_H(Q) > 0, \quad \lambda_S(Q) > 0, \quad \kappa(Q) + 2\sqrt{\lambda_H(Q)\lambda_S(Q)} > 0$$

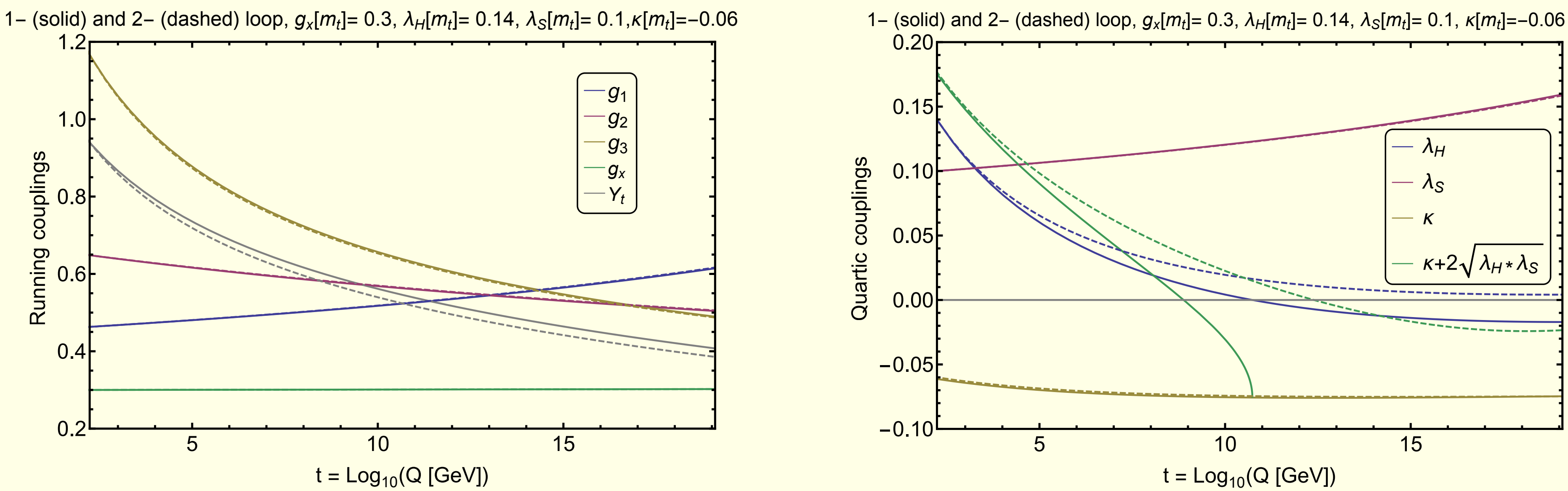

Figure 11: Running of various parameters at 1- and 2-loop, in solid and dashed lines respectively. For this choice of parameters $\lambda_H(Q) > 0$ at 2-loop (right panel blue) but not at 1-loop. $\lambda_S(Q)$ is always positive (right panel red), running of $\kappa(Q)$ is very limited, however the third positivity condition $\kappa(Q) + 2\sqrt{\lambda_H(Q)\lambda_S(Q)} > 0$ is violated at higher scales even at 2-loops (right panel green).

The mass of the Higgs boson is known experimentally therefore within *the SM* the initial condition for running of $\lambda_H(Q)$ is fixed

$$\lambda_H(m_t) = M_{h_1}^2/(2v^2) = \lambda_{SM} = 0.13$$

For VDM this is not necessarily the case:

$$M_{h_1}^2 = \lambda_H v^2 + \lambda_S v_S^2 \pm \sqrt{\lambda_S^2 v_S^4 - 2\lambda_H \lambda_S v^2 v_S^2 + \lambda_H^2 v^4 + \kappa^2 v^2 v_S^4}.$$

VDM:

- Larger initial values of λ_H such that $\lambda_H(m_t) > \lambda_{SM}$ are allowed delaying the instability (by shifting up the scale at which $\lambda_H(Q) < 0$).

- Even if the initial λ_H is smaller than its SM value, $\lambda_H(m_t) < \lambda_{SM}$, still there is a chance to lift the instability scale if appropriate initial value of the portal coupling $\kappa(m_t)$ is chosen.

$$\beta_{\lambda_H}^{(1)} = \beta_{\lambda_H}^{SM\ (1)} + \kappa^2$$

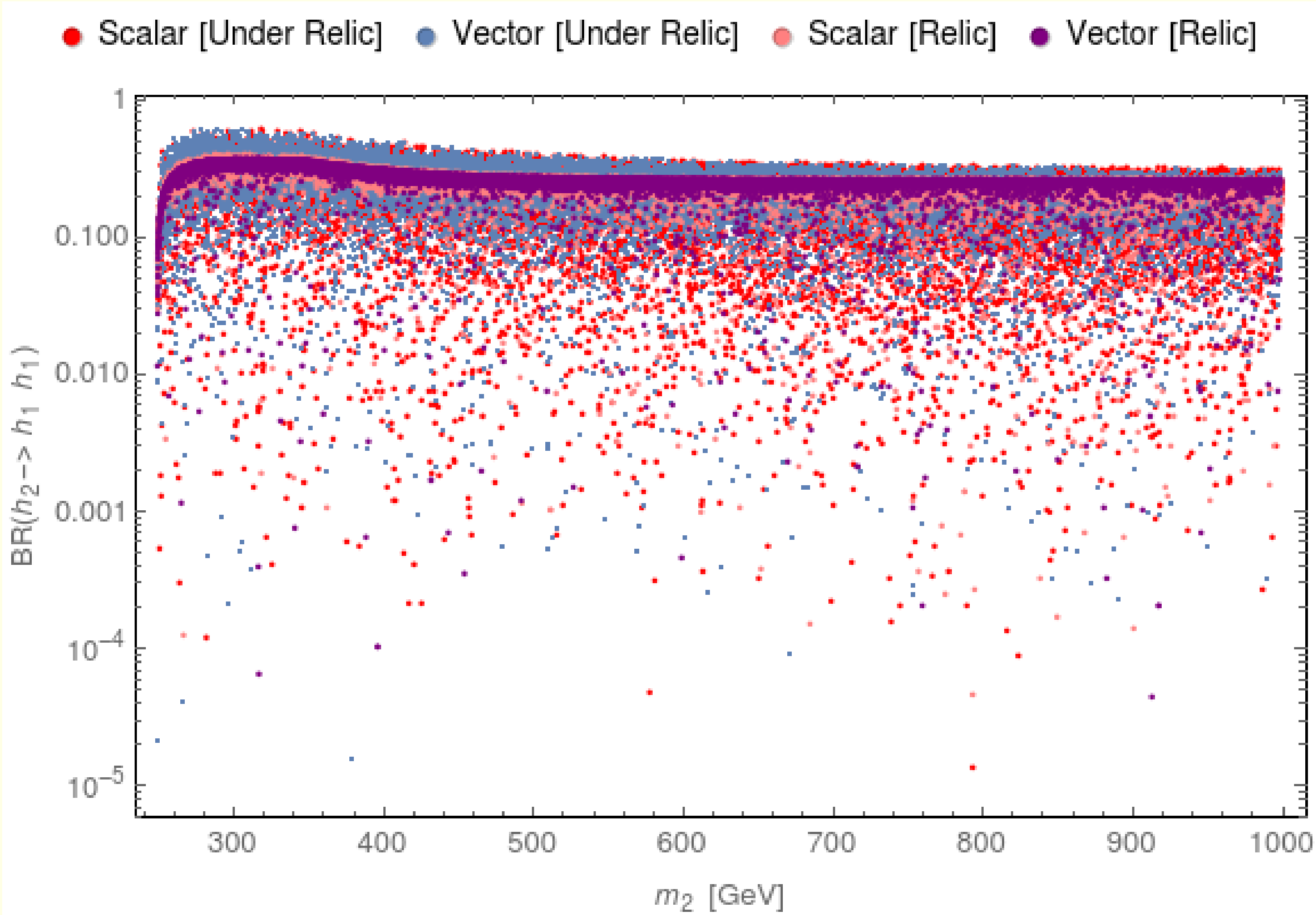

Figure 12: Branching ratio of second Higgs vs. mass of second Higgs. Scalar model in red, vector model in blue.

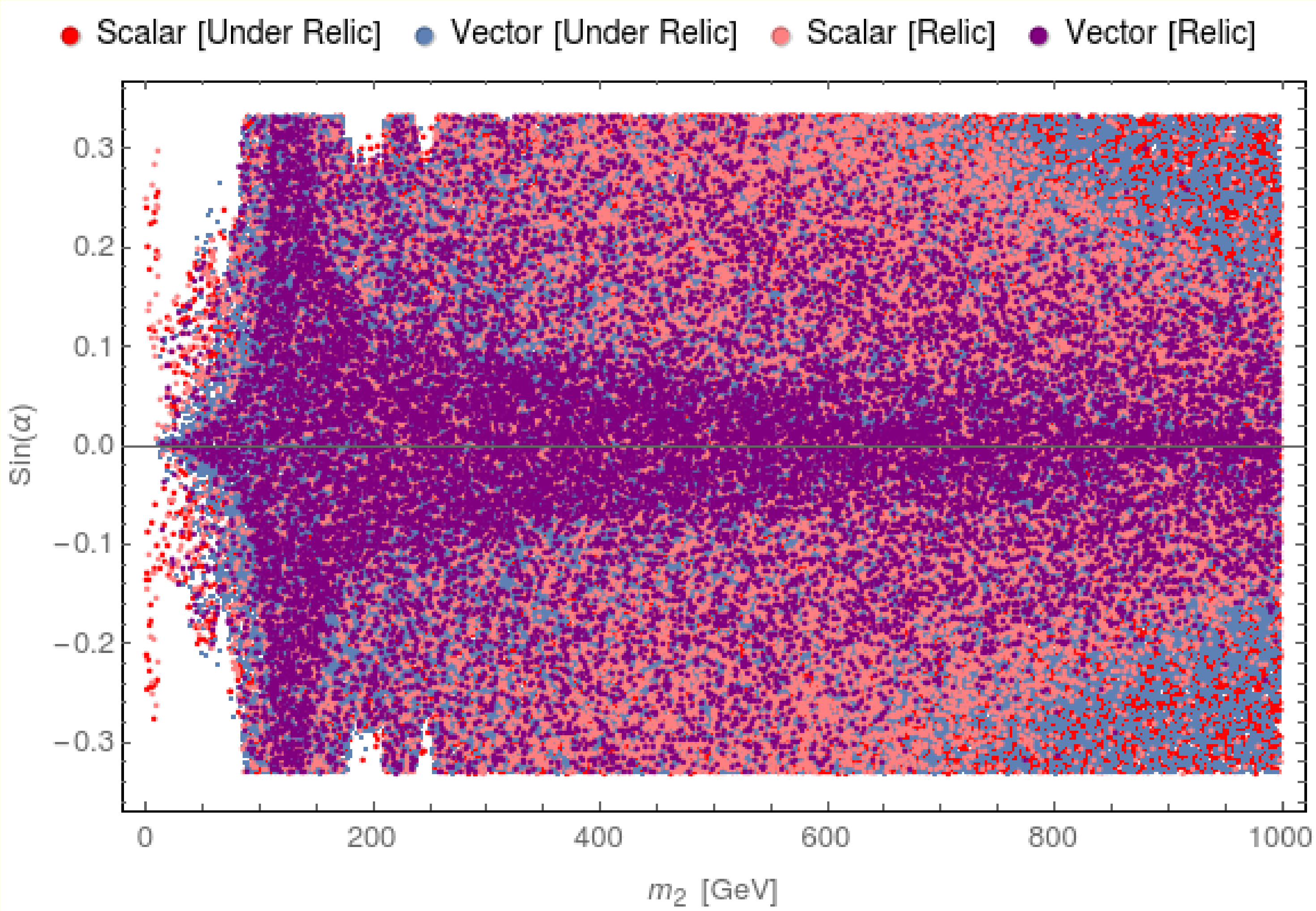

Figure 13: $\sin\alpha$ versus m_2.

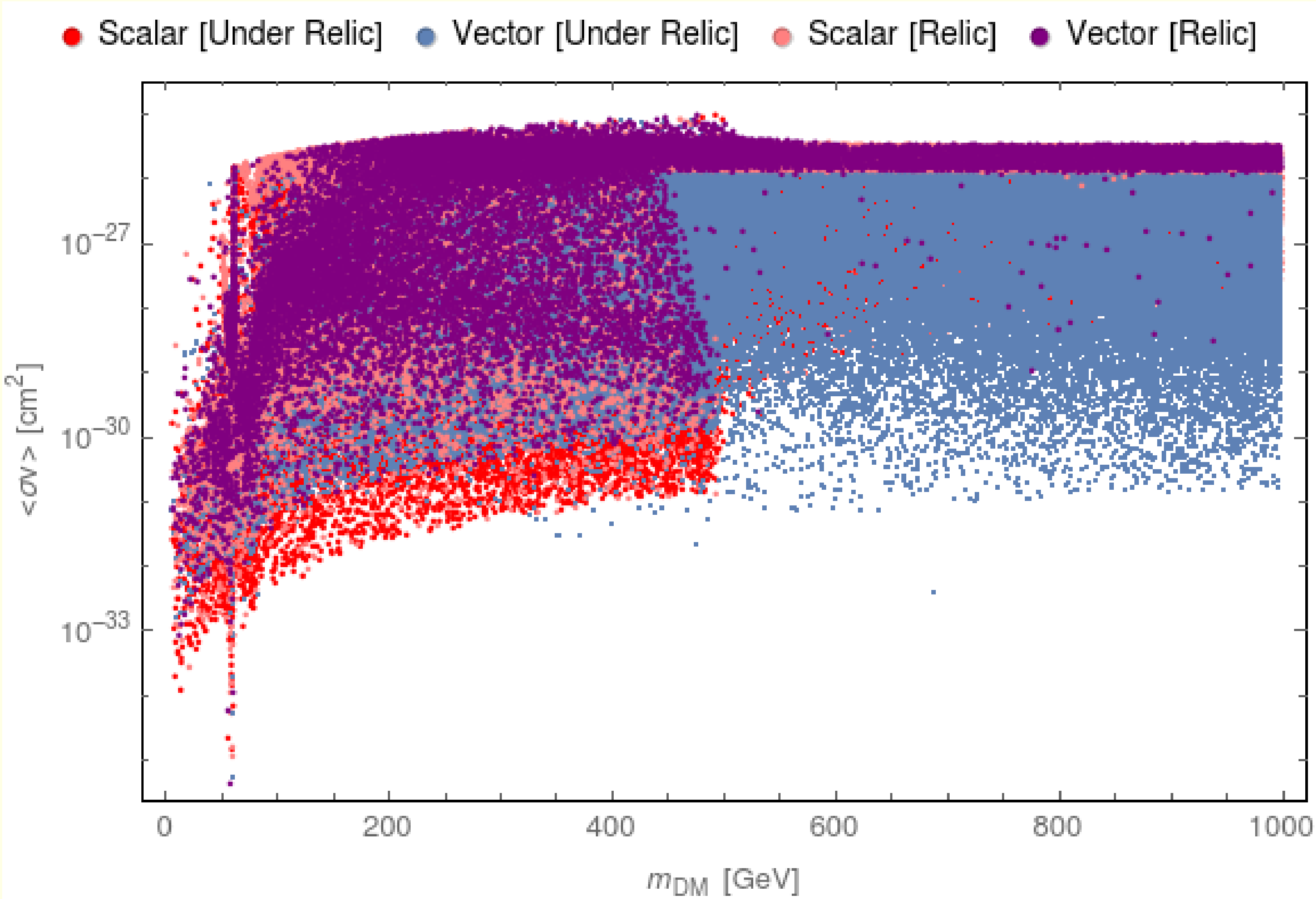

Figure 14: Dark matter-nucleon cross section versus m_{DM}.

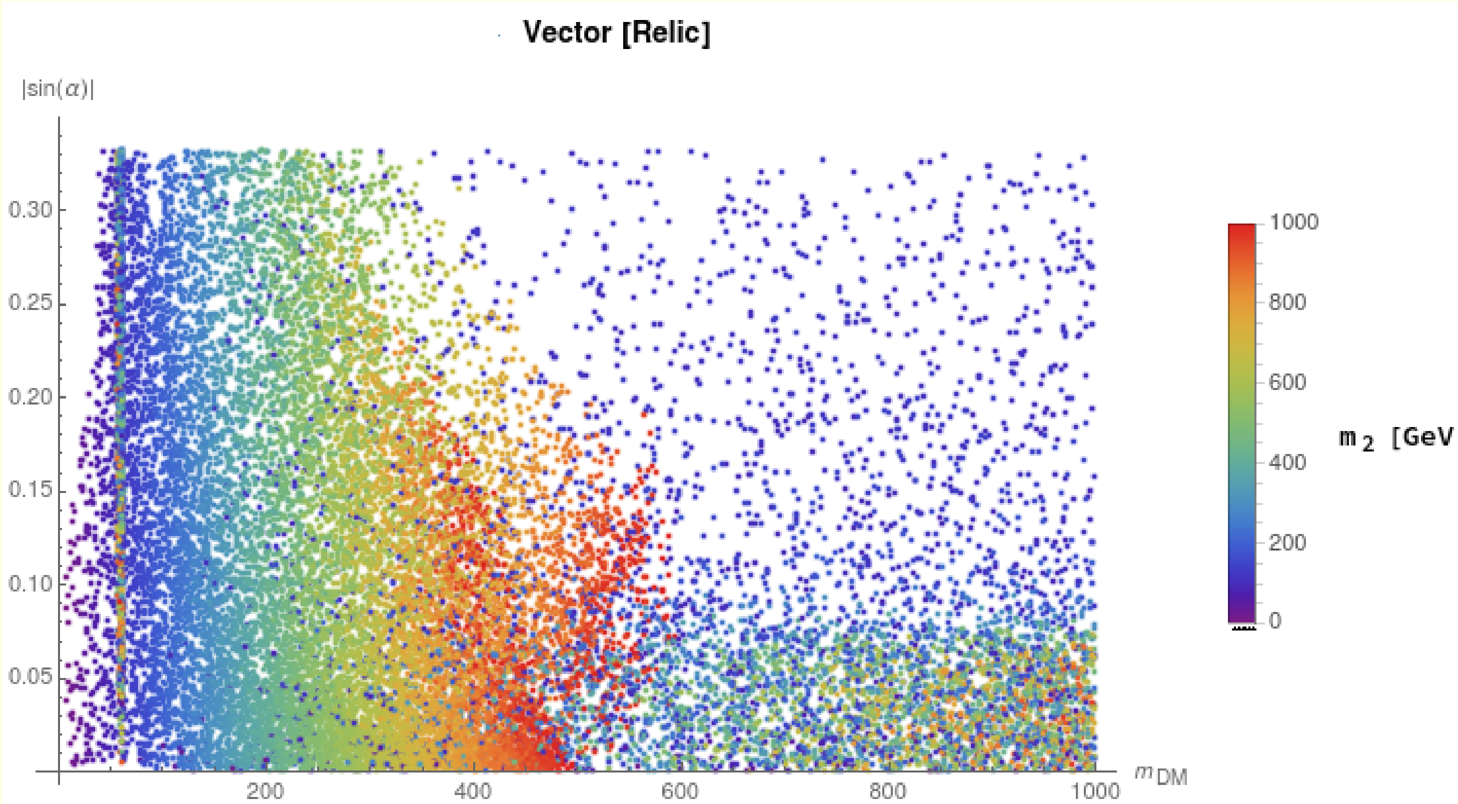

Figure 15: $\sin\alpha$ versus m_2 for VDM. Coloring with respect to $\sin\alpha$.

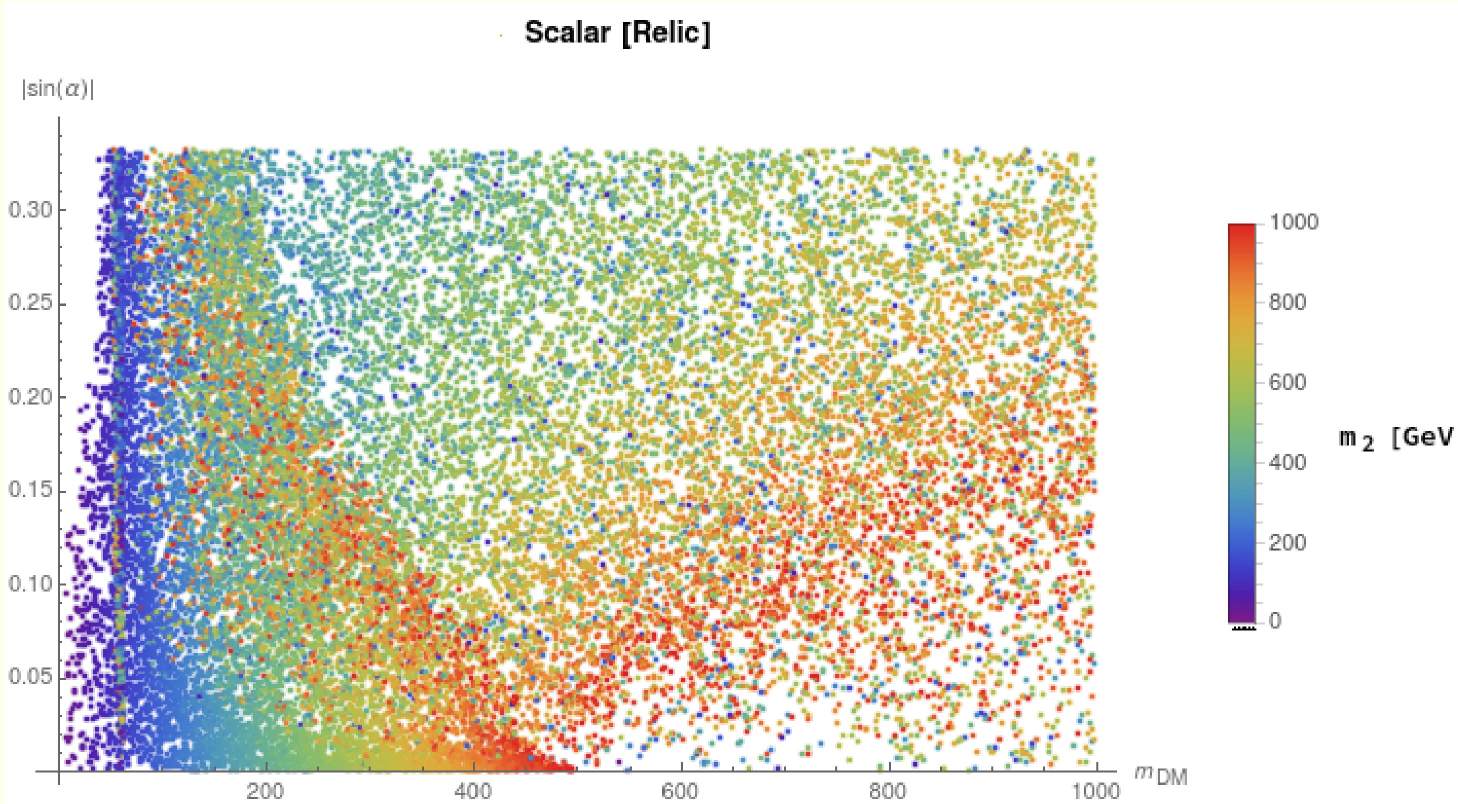

Figure 16: $\sin\alpha$ versus m_2 for SDM. Coloring with respect to $\sin\alpha$.